Magnon Squeezing in an Antiferromagnet: Reducing the Spin Noise below the Standard Quantum Limit

Jimin Zhao,[1] A.V. Bragas,[1,*] D. J. Lockwood,[2] and R. Merlin[1]

[1]*Focus Center and Department of Physics, The University of Michigan, Ann Arbor, Michigan, 48109-1120, USA*
[2]*Institute for Microstructural Sciences, National Research Council, Ottawa K1A 0R6, Canada*

(Received 17 November 2003; published 2 September 2004)

We report the first experimental demonstration of quantum squeezing of a collective spin-wave excitation (magnon) using femtosecond optical pulses to generate correlations involving pairs of spins in an antiferromagnetic insulator MnF_2. In the squeezed state, the fluctuations of the magnetization of a crystallographic unit cell vary periodically in time and are reduced below that of the ground-state quantum noise.

DOI: 10.1103/PhysRevLett.93.107203 PACS numbers: 75.90.+w, 42.50.Dv, 42.65.Dr, 78.47.+p

The fact that noise is inherent to quantum systems has been known since Heisenberg postulated the uncertainty principle in 1927 [1]. Remarkably, despite this fact, the noise of a *given* quantum observable can in theory be eliminated entirely through quantum squeezing [2]. Quantum squeezing refers to a state whereby noise in one variable is reduced at the expense of enhancing the noise of its conjugate variable. The terminology originates from quantum optics, and it is usually applied to a system of noninteracting bosons. Squeezed states have only been achieved fairly recently and were first demonstrated for the electromagnetic field (photons) in 1985 [3]. Nonlinear interactions of light with passive and active atomic media have been successfully used to generate squeezed photons, opening possibilities for essentially noiseless optical communications and precision measurements [4,5]. The electromagnetic field is now not the only system that has been squeezed. In the past decade, squeezed states of vibrational degrees of freedom have been experimentally demonstrated for molecules [6] and solids [7,8] and, more recently, squeezed atomic spin states have also been achieved [9–13]. Because spin squeezing is closely related to quantum entanglement, squeezed states hold promise for applications in quantum computing [14]. In addition, thermal squeezing is also possible for classical objects [15].

Impulsive stimulated second-order (inelastic light) Raman scattering (RS) has been shown to be a practical means to generate squeezed states for phonons in solids [7,8,16]. Second-order Raman coupling between the incident light and lattice vibrations is proportional to the square of the phonon amplitude. This interaction gives rise to squeezing because it represents a change in the frequency of the harmonic oscillator for the duration of the incident light pulse and, as such, it is a parametric perturbation. Here, we concern ourselves with noise in a magnetically ordered solid for which the low-lying spin excitations are bosons known simply as spin waves or magnons. Such collective excitations are commonly observed by RS [17]. Thus, as for phonons, we achieve magnon squeezing by means of impulsive stimulated second-order RS. Magnon squeezing in antiferromagnets results in a reduction of the noise of the crystallographic unit cell magnetization.

Manganese difluoride MnF_2 crystallizes in the tetragonal rutile structure (of D_{4h} symmetry) and becomes antiferromagnetic below the Néel temperature $T_N = 68$ K [18]. In the ordered state, there are two spin sublattices α and β, in which the Mn^{2+} spins align "up" and "down" along the fourfold axis of symmetry [001]. Ignoring the weaker intrasublattice exchange and the magnetic anisotropy, the spin dynamics of MnF_2 is well described by the one-parameter Hamiltonian [17,18]

$$H_0 = J \sum_{\langle u,\nu \rangle} \mathbf{S}_{u,\alpha} \cdot \mathbf{S}_{\nu,\beta}. \tag{1}$$

Here, J is the dominant intersublattice exchange constant associated with the interaction between a given Mn^{2+} ion and its eight next-nearest neighbors, and the sum runs over pairs of next-nearest neighbors. In the harmonic approximation

$$H_0 \approx \sum_{\mathbf{q}} \hbar \Omega_{\mathbf{q}} (a^+_{\uparrow\mathbf{q}} a_{\uparrow\mathbf{q}} + a^+_{\downarrow\mathbf{q}} a_{\downarrow\mathbf{q}}), \tag{2}$$

where $a^+_{\uparrow\mathbf{q}}$ and $a^+_{\downarrow\mathbf{q}}$ ($a_{\uparrow\mathbf{q}}$ and $a_{\downarrow\mathbf{q}}$) are creation (annihilation) operators for magnons of wave vector $\mathbf{q}$ and frequency $\Omega_{\mathbf{q}}$ belonging to the two degenerate branches labeled $\uparrow$ (up) and $\downarrow$ (down) [19,20]. For wave vectors near the edge of the Brillouin zone, the excitations generated by $a^+_{\uparrow\mathbf{q}}$ ($a^+_{\downarrow\mathbf{q}}$) propagate mainly on the α (β) sublattice (a magnon of arbitrary $\mathbf{q}$ generally perturbs both sublattices) [17].

Phenomenologically, the Raman coupling between magnons and light can be expanded in powers of the spins of the magnetic ions [17]. In MnF_2, and most antiferromagnets, the first-order contribution relying on spin-orbit coupling is far less important than the second-order term which results from excited-state exchange and leads to RS by magnon pairs. Let $\mathbf{E}(\mathbf{r}, t) = E(e_x, e_y, e_z)$ be the position- and time-dependent electric field. From symmetry considerations, the two-magnon interaction rele-

vant to stimulated RS can be written as [19,20]

$$V = \frac{E^2}{2} \sum_{\langle u,\nu \rangle} \Xi(u,\nu)(S^+_{u,\alpha} S^-_{\nu,\beta} + S^-_{u,\alpha} S^+_{\nu,\beta} + \gamma S^z_{u,\alpha} S^z_{\nu,\beta}), \quad (3)$$

where $S^{\pm} = S_x \pm iS_y$ and $\Xi = \kappa_1(e_x e_x + e_y e_y) + \kappa_2 e_z e_z + 2\kappa_3[e_x e_y \operatorname{sgn}\rho_x \operatorname{sgn}\rho_y] + 2\kappa_4[e_y e_z \operatorname{sgn}\rho_y \operatorname{sgn}\rho_z + e_x e_z \operatorname{sgn}\rho_x \operatorname{sgn}\rho_z]$. Here γ is an anisotropy parameter, $\rho = (\rho_x, \rho_y, \rho_z)$ is a vector connecting a given ion with its next-nearest neighbors in the opposite sublattice, and κ_m ($m = 1$–4) are magneto-optic constants associated with the Raman tensors of symmetry A_{1g} (κ_1 and κ_2), B_{2g} (κ_3), and E_g (κ_4). The relative magnitudes of the latter can be inferred from spontaneous Raman data which give $[\kappa_1/\kappa_3] = 0.14$, $[\kappa_2/\kappa_3] = 0.32$, and $[\kappa_4/\kappa_3] = 0.66$ [20]. In our experiments, the only symmetry that matters is B_{2g}.

It is straightforward to express V in terms of magnon variables. For our purposes, however, it is sufficient to consider only zone-edge excitations since the magnon density of states is strongly peaked at van Hove singularities close to the Brillouin zone boundary. Writing $V = \sum_{\mathbf{q}} V_{\mathbf{q}}$, we obtain for $\mathbf{q}$ near the edge $V_{\mathbf{q}} \approx SE^2 \Delta_{\mathbf{q}} (a^+_{\downarrow\mathbf{q}} a^+_{\uparrow-\mathbf{q}} + a_{\downarrow\mathbf{q}} a_{\uparrow-\mathbf{q}})$ where $S = 5/2$ is the spin of Mn^{2+} and $\Delta_{\mathbf{q}}$ is a weighting factor that generally depends on the field polarization and the appropriate combination of magneto-optic coefficients. For the B_{2g} term, $\Delta_{\mathbf{q}} = -8\kappa_3 \sin(q_x a/2) \sin(q_y a/2) \cos(q_z c/2)$ where a and c are the lattice constants [19,20]. This geometry favors the M point of the Brillouin zone and gives the largest contribution to two-magnon RS [19,20].

The coupling defined by V describes a time-dependent pairwise interaction between magnons. To describe the effect of a laser pulse on the magnetic system, we consider the impulsive limit, i.e., an optical pulse of width $\tau \ll \Omega^{-1}$, and, for simplicity, we take the speed of light $c_L \to \infty$. Then, the field can be treated as an instantaneous and position-independent perturbation $E^2 \approx (4\pi I/n_R c_L)\delta(t)$ where n_R is the refractive index and I is the integrated intensity of the pulse. Let Ψ_0 be the wave function of the whole crystal just before the pulse strikes. A simple integration of the Schrödinger equation gives, for $t > 0$ [7],

$$\Psi = e^{iH_0 t/\hbar} \exp\left[-i \sum_{\mathbf{q}} \frac{4\pi SI}{n_R c_L \hbar} \Delta_{\mathbf{q}} (a^+_{\downarrow\mathbf{q}} a^+_{\uparrow-\mathbf{q}} + a_{\downarrow\mathbf{q}} a_{\uparrow-\mathbf{q}}) \right] \Psi_0. \quad (4)$$

At zero temperature, Ψ_0 is the magnetic ground state, and this expression becomes identical to that describing two-mode squeezed states [2]. After some algebra, we obtain, to lowest order in the intensity of the pulse,

$$\langle \Psi | (a^+_{\downarrow\mathbf{q}} a^+_{\uparrow-\mathbf{q}} + a_{\downarrow\mathbf{q}} a_{\uparrow-\mathbf{q}}) | \Psi \rangle \approx -\frac{8\pi SI}{n_R c_L \hbar} \Delta_{\mathbf{q}} \sin(2\Omega_{\mathbf{q}} t). \quad (5)$$

Hence, Eq. (4) represents a state in which there exists a time-varying correlation between magnons of opposite wave vectors that belong to the two degenerate branches.

Data were obtained from a $5.5 \times 5.8 \times 6.0$ mm^3 single crystal of MnF_2. Time-domain measurements were performed at 4 K using a standard pump-probe setup in a transmission geometry that allows only B_{2g} excitations. We used 50 fs pulses generated by an optical parametric amplifier at a repetition rate of 250 kHz and 534 nm central wavelength, which were focused onto a common 30-μm-diameter spot. The average power for the pump and probe pulses was, respectively, 13 and 3 mW. Light penetrated the crystal along the [001] direction. The pump pulses were polarized along the [110] direction. This geometry couples to modes of both A_{1g} and B_{2g} symmetry. The probe polarization was set at an angle of 45° with respect to the polarization of the pump. The transmitted probe pulses were divided into two beams, one polarized parallel and the second one perpendicular to the pump polarization. These beams were sent to two separate detectors. It can be shown that the difference between the signals recorded by these detectors is equal to twice the differential transmission for the B_{2g} geometry while the subtraction eliminates the isotropic A_{1g} contribution. The stronger pump pulse drives the crystal into the time-varying squeezed state [Eq. (4)], and the concomitant time-varying refractive index scatters the weaker probe pulse that follows behind. The signal of interest is the transmitted intensity of the probe beam as a function of the time delay between the two pulses. Using Eq. (5) and well-known results for coherent phonons [21], we obtain the following expression for the differential transmission:

$$\Delta T/T \approx \frac{\ell I}{\hbar N \nu_C} \left(\frac{8\pi S}{n_R c_L} \right)^2 \sum_q \Omega_q \Delta^2_{\mathbf{q}} \cos(2\Omega_q t), \quad (6)$$

which is valid for probe pulses of negligible width. Here ℓ is the length of the sample, N is the number of unit cells, and ν_C is the cell volume.

The time-domain data of Fig. 1 show well-resolved oscillations. After removal of the so-called coherent artifact at $t = 0$, we used linear prediction (LP) methods [22] to determine the number of oscillators and their parameters. As shown in the Fourier transform spectrum of the inset, this procedure gives three modes. Their positions, at ~100, 347, and 481 cm^{-1}, are in excellent agreement with those of, respectively, the two-magnon feature and the Raman-allowed phonons of symmetries A_{1g} and B_{2g} [23]. Based on this result and the previous discussion, the ~100 cm^{-1} oscillations are ascribed to a two-magnon squeezed state, whereas the other two features are assigned to coherent phonons. The observation of the A_{1g} mode is attributed to a polarization leakage in the experiment. While A_{1g} excitations are not nominally allowed in our configuration, the Raman cross section for the 347 cm^{-1} phonon is so large that it cannot be entirely suppressed by our method.

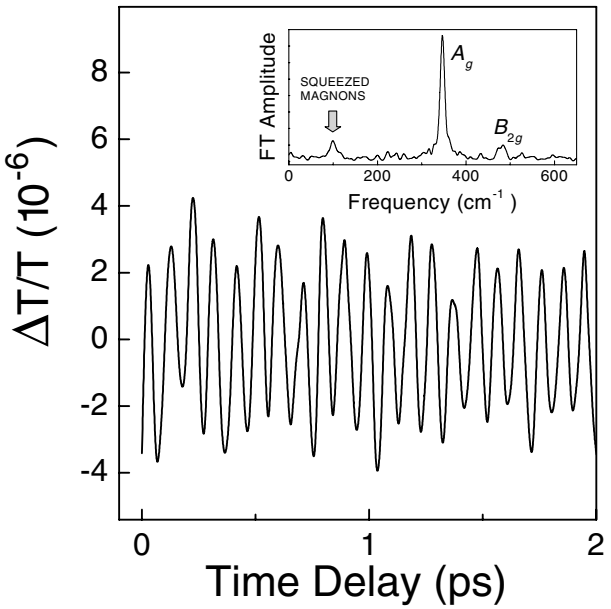

FIG. 1. Relative differential transmission as a function of pump-probe delay. The Fourier transform spectrum in the inset shows peaks due to coherent two-magnon excitations (squeezed magnons) and coherent phonons.

The two-magnon oscillations are reproduced in Fig. 2(a) after numerical subtraction of the signal due to the phonons. As shown in Fig. 2(b), the Fourier transform of the LP fit to the time-domain data compares well with the measured two-magnon Raman spectrum. In Fig. 2(c), we show the magnon dispersion curve [18], which supports our contention that the pump-probe signal is dominated by magnon pairs at the zone boundary. The magnetic oscillations do not show the phase predicted by Eq. (6) at zero time delay. We believe that this discrepancy reflects simply the fact that Eq. (3) and, therefore, Eq. (6) apply to transparent materials, whereas the wavelength of our laser falls within a broad absorption band of MnF_2 [24]. In such a case, it is well known that the phase of the coherent oscillations can have arbitrary values [25]. Further support for this interpretation is the observation that the two-magnon signal does not vanish in integrated transmission measurements since the sample behaves as a frequency-dependent filter [21].

The above arguments support our claim that the coherence responsible for the oscillations of Fig. 2 is that of a magnon squeezed state, but we have not yet given a physical interpretation of such a state. Let $\mathbf{m}_l$ be the local magnetization operator. In the following we show that magnon squeezing is tantamount to time-dependent fluctuations of the local magnetization noise $\sigma_m = \sqrt{\langle \mathbf{m}_l^2 \rangle}$ (note that $\langle \mathbf{m}_l \rangle = 0$ always, and that $\langle \mathbf{m}_l^2 \rangle$ has the same value for all cells). The proof is relatively simple. Writing $\mathbf{m}_l = g\mu_B(\mathbf{S}_{l,\alpha} + \mathbf{S}_{l,\beta})$ where the spins belong to the same cell, g is the Landé factor, and μ_B is the Bohr magneton, we have

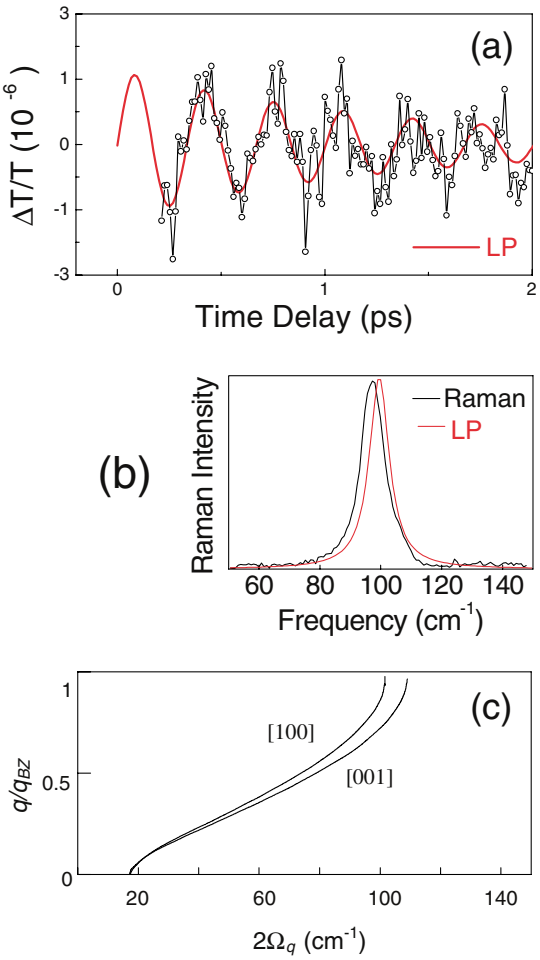

FIG. 2 (color). (a) Pump-probe data showing two-magnon oscillations. The LP fit is shown in red. (b) Comparison between the Fourier transform of the LP fit (red) and the Raman spectrum recorded at 3 K using 140 mW of 514.5 nm Ar^+ laser light. (c) Magnon dispersion for wave vectors in the [100] and [001] directions (from Ref. [18]). To compare with the Raman experiments, the frequency scale has been multiplied by a factor of 2.

$$\frac{1}{2}\sum_l \langle \mathbf{m}_l^2 \rangle / (g\mu_B)^2 = NS(S+1) + \sum_{\mathbf{q}} \langle \mathbf{S}_\alpha(\mathbf{q}) \cdot \mathbf{S}_\beta(-\mathbf{q}) \rangle, \tag{7}$$

where N is the total number of unit cells and $\mathbf{S}_{\alpha/\beta}(\mathbf{q}) = \sum \mathbf{S}_{l,\alpha/\beta} \exp(i\mathbf{q} \cdot \mathbf{r}_{l,\alpha/\beta})/N^{1/2}$ (the sum is over all sites of the corresponding sublattice). From Eqs. (4) and (7), we obtain in the harmonic approximation and, for $I \to 0$,

$$\sigma_m(t) \approx \sigma_m^0 \left[1 + \frac{4\pi I S}{N n_R c_L \hbar} \sum_q \Delta_{\mathbf{q}} \sin(2\Omega_q t) \right], \tag{8}$$

where $\sigma_m^0 = (2S)^{1/2} g\mu_B$ is the ground-state noise. If we compare this expression with Eq. (6), it is clear that the amplitude of the coherent oscillations is proportional to the change in the local magnetization noise. In essence, the noise is being controlled by the laser-induced

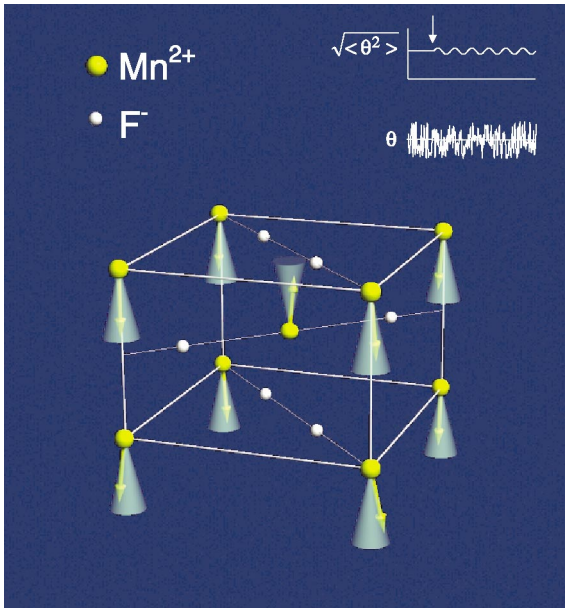

FIG. 3 (color). Schematic representation of magnon squeezing in MnF_2. The arrows and cones attached to the manganese ions represent, respectively, the spins and their angular fluctuations at zero temperature. The inset shows the time dependence of the noise (represented by the angle θ, which fluctuates about an expectation value of zero) and the square root of the expectation value of θ^2, which is finite. The arrow indicates the time at which the laser pulse impinges on the solid.

refractive-index modulation. Since both Eqs. (6) and (8) are dominated by contributions from magnons near the M point of the Brillouin zone, of frequency Ω_M, we obtain approximately

$$\sigma_m(t) \approx \sigma_m^0[1 + \xi(\Delta T/T)|_{\max} \sin(2\Omega_M t)], \qquad (9)$$

where $\xi = v_C n_R c_L/(16\pi \ell S \Omega_M \Delta_M)$. A graphic representation of a squeezed state is shown in Fig. 3. Instead of the local magnetization itself, we use the angle θ defined as $\cos\theta = -\mathbf{S}_{l,\alpha} \cdot \mathbf{S}_{l,\beta}/S(S+1)$ to represent the noise, noting that

$$\sigma_m \approx g\mu_B \sqrt{S(S+1)} \sqrt{\langle\theta^2\rangle}. \qquad (10)$$

Thus, pictorially, the laser excited spin squeezing results in a sinusoidal modulation of $\sqrt{\langle\theta^2\rangle}$, which reflects the laser-induced control over the local magnetization fluctuations.

To provide a quantitative estimate of the squeezing, we write Eq. (3) as $V = E^2 \sum_{\mathbf{q}} \Theta(\mathbf{q}) \mathbf{S}_\alpha(\mathbf{q}) \cdot \mathbf{S}_\beta(-\mathbf{q})$ which shows that, except for the weighting factors $\Theta(\mathbf{q})$, light couples directly to fluctuations of the local magnetization. Given that contributions near the Brillouin zone boundary are dominant, $V \approx E^2 \tilde{\Theta} N \hbar^2 [(\sigma_m/g\mu_B)^2/2 - S(S+1)]$ where $\tilde{\Theta}$ denotes an average value at the zone boundary. By evaluating Eq. (9) with the experimental values, one can estimate the noise reduction. The thermal noise at 4 K is approximately the product of $\sigma_m(0)$ times twice the Bose factor at $\hbar\Omega_M$ [8]. Under our experimental conditions, the term multiplying $\sin(2\Omega_M t)$ in Eq. (9) is $\sim 2 \times 10^{-5}$ while the thermal contribution to the noise is $\sim 3 \times 10^{-8}$. Clearly, the noise level in the local magnetization has been reduced below the quantum limit through magnon squeezing.

This work was supported by the NSF under Grants No. PHY 0114336 and No. DMR 0072897, and by the AFOSR under Contract No. F49620-00-1-0328 through the MURI program. One of us (A. V. B.) acknowledges partial support from CONICET, Argentina.

*Present address: FCEyN, Universidad de Buenos Aires, Ciudad Universitaria, 1428 Buenos Aires, Argentina.

[1] W. Heisenberg, Z. Phys. **43**, 172 (1927).
[2] D. F. Walls and G. J. Milburn, *Quantum Optics* (Springer, Berlin, 1994).
[3] R. E. L. Slusher *et al.*, Phys. Rev. Lett. **55**, 2409 (1985).
[4] R. Loudon and P. L. Knight, J. Mod. Opt. **34**, 709 (1987).
[5] L. Davidovich, Rev. Mod. Phys. **68**, 127 (1996).
[6] T. J. Dunn, J. N. Sweetser, I. A. Walmsley, and C. Radzewicz, Phys. Rev. Lett. **74**, 884 (1995).
[7] G. A. Garrett *et al.*, Science **275**, 1638 (1997).
[8] G. A. Garrett *et al.*, Opt. Express **1**, 385 (1997); A. Bartels, T. Dekorsy, and H. Kurz, Phys. Rev. Lett. **84**, 2981 (2000); A. G. Stepanov, J. Hebling, and J. Kuhl, Phys. Rev. B **63**, 104304 (2001).
[9] A. Kuzmich, L. Mandel, and N. P. Bigelow, Phys. Rev. Lett. **85**, 1594 (2000).
[10] J. Hald, J. L. Sørensen, C. Schori, and E. S. Polzik, Phys. Rev. Lett. **83**, 1319 (1999).
[11] D. J. Wineland, J. J. Bollinger, W. N. Itano, and D. J. Heinzen, Phys. Rev. A **50**, 67 (1994).
[12] B. Julsgaard, A. Kozhekin, and E. S. Polzik, Nature (London) **413**, 400 (2001).
[13] A. Dantan *et al.*, Phys. Rev. A **67**, 045801 (2003).
[14] X. Wang and B. C. Sanders, Phys. Rev. A **68**, 012101 (2003).
[15] B. Yurke *et al.*, Phys. Rev. Lett. **60**, 764 (1988).
[16] A. P. Mayer, R. K. Wehner, and A. A. Maradudin, Phys. Rev. B **62**, 5513 (2000), and references therein.
[17] M. G. Cottam and D. J. Lockwood, *Light Scattering in Magnetic Solids* (Wiley, New York, 1986).
[18] A. Okasaki, K. C. Turberfield, and R. W. H. Stevenson, Phys. Lett. **8**, 9 (1964).
[19] P. A. Fleury and R. Loudon, Phys. Rev. **166**, 514 (1968).
[20] D. J. Lockwood and M. G. Cottam, Phys. Rev. B **35**, 1973 (1987).
[21] R. Merlin, Solid State Commun. **102**, 207 (1997).
[22] H. Barkhuijsen, R. De Beer, W. M. M. J. Bovée, and D. van Ormondt, J. Magn. Reson. **61**, 465 (1985).
[23] S. P. S. Porto, P. A. Fleury, and T. C. Damen, Phys. Rev. **154**, 522 (1967).
[24] T. Tsuboi and P. Ahmet, Phys. Rev. B **45**, 468 (1992).
[25] T. E. Stevens, J. Kuhl, and R. Merlin, Phys. Rev. B **65**, 144304 (2002).